Alternative Neutralization Technologies Enabling the Use of Exotic Propellants in Electric Propulsion

IEPC-2017-251

Presented at the 35th International Electric Propulsion Conference
Georgia Institute of Technology • Atlanta, Georgia • USA
October 8 – 12, 2017

Antonio Gurciullo* and Andrea Lucca Fabris†
University of Surrey, Guildford, GU2 7XH, United Kingdom

and

Aaron Knoll‡
Imperial College London, London, SW7 2AZ, United Kingdom

Abstract: In this paper we present the design and test campaign results of two plasma cathodes for electric propulsion applications. One cathode is based on a Hall-type discharge operated in DC. Three magnetic topologies have been tested in order to govern the discharge and the electron extraction with this neutralizer. The second cathode exploits a planar magnetron discharge operated in DC. Preliminary results of extraction tests involving atomic and molecular gases are presented. It is shown that the presence of open-loop Hall currents and null magnetic regions created by four arc magnets whose axial polarity is alternated may increase extraction performance of the Hall-type neutralizer. It is also shown that the extraction characteristics of the planar magnetron neutralizer are qualitatively similar to those of the Hall-type neutralizer.

Nomenclature

α	=	extraction efficiency
$\boldsymbol{B}$	=	magnetic field
C	=	constant (0.07174 A/sccm)
$D_\perp$	=	electron diffusion constant across magnetic field
D	=	electron diffusion constant along magnetic field
DC	=	direct current
e	=	elementary charge
$\boldsymbol{E}$	=	electric field
ERC	=	electron cyclotron resonance
H_p	=	partial power efficiency
I_D	=	discharge current
I_{extr}	=	extracted electron current
J_i	=	ion current density
$\dot{m}_g$	=	gas flow rate
M_i	=	ion mass
ω_c	=	gyration frequency

* PhD Candidate, Surrey Space Centre, a.gurciullo@surrey.ac.uk.
† Lecturer in Space Propulsion, Surrey Space Centre, a.luccafabris@surrey.ac.uk.
‡ Senior Lecturer in Spacecraft Engineering, Department of Aeronautics, a.knoll@imperial.ac.uk.

P_D	=	discharge power
PPU	=	power processing unit
R	=	plasma ring radius
R_c	=	magnetic field line curvature
r_{ce}	=	electron Larmor radius
RF	=	radio frequency
R_{sh}	=	resistance of shunt resistor
s	=	sheath thickness
sccm	=	standard cubic centimetre per minute
τ_m	=	characteristic time between electron momentum transfer collisions
U	=	utilization factor
V_D	=	discharge voltage
V_{sh}	=	voltage drop across shunt resistor
$v_{E\times B}$	=	particle drift velocity due to $\boldsymbol{E}\times\boldsymbol{B}$ field
w	=	plasma ring width

I. Introduction

CONVENTIONAL neutralizers, such as hollow cathodes and dispenser cathodes, provide electrons by thermionic emission utilizing specially formulated low work function materials, such as barium oxide (BaO) and lanthanum hexaboride (LaB_6) inserts . Thermionic emission is degraded by electronegative gases that are chemically adsorbed on the insert material and cause an increase of its work function. This process is referred as cathode poisoning.[1,2] At the same time, the research community has shown a growing interest in operating plasma thrusters with a wide range of unconventional propellants, including electronegative gases and condensable propellants. In this research frame, the behaviour and performance of plasma thrusters have been characterized for a selection of non-noble gases,[3,4] and conventional neutralizers have been tested with oxygen, CO_2 and air.[2] However, above a partial pressure threshold of those compounds cathode poisoning is triggered.

Since late 1970s, alternative methods in which electrons are mainly created in the bulk plasma rather than in surface interactions have been explored. Cathodes adopting these methods are usually referred as plasma cathodes.[5] In most of plasma cathodes, plasma is created by means of radio frequency (RF),[6] microwave,[7] electron cyclotron resonance (ECR),[8] or helicon waves.[9] In this paper, two direct current (DC) plasma cathode concepts are presented. Both neutralizers have been tested with noble gas and molecular propellants. In section II the working principles and the designs of the plasma sources are presented. Section III covers the experimental setup, and in Section IV the results of the test campaign are shown and discussed. Finally, section V presents the conclusions.

II. Neutralizer Concepts

The two plasma cathodes presented in this paper are a Hall-type neutralizer and a planar magnetron type, both operated in DC. The following sections present the design and working principle of the neutralizers.

A. Hall-Type Neutralizer

The Hall-type neutralizer is based on a DC plasma discharge enhanced by a closed-loop $\boldsymbol{E}\times\boldsymbol{B}$ electron drift. The $\boldsymbol{E}\times\boldsymbol{B}$ drift is a well-known charged-particle dynamic generated by the simultaneous action of an electric field $\boldsymbol{E}$ and a magnetic field $\boldsymbol{B}$. The resulting particle drift velocity is determine by the relation:

$$v_{E\times B} = \boldsymbol{E}\times\boldsymbol{B}/B^2 \tag{1}$$

This phenomenon is exploited in Hall plasma sources in order to enhance the electron resident time within a discharge channel while increasing the ionization efficiency. For the typical magnetic field range applied in these devices, only electron dynamics is influenced by the magnetic field, whereas ions are unmagnetized. The effect of the magnetic field on ion dynamics is usually indirect and is generated by the electric field resulting from the decreased electron mobility in the strongest magnetic field region.

The neutralizer is made of two fundamental stages: a discharge volume, where ionization of the neutral gas due to $\boldsymbol{E}\times\boldsymbol{B}$ drift takes place, and an acceleration volume, where electrons diffuse toward and are extracted through an orifice bore on an extraction plate. The electric field is applied along the radial direction and the magnetic field is applied along the axial one, generating an azimuthal electron drift.

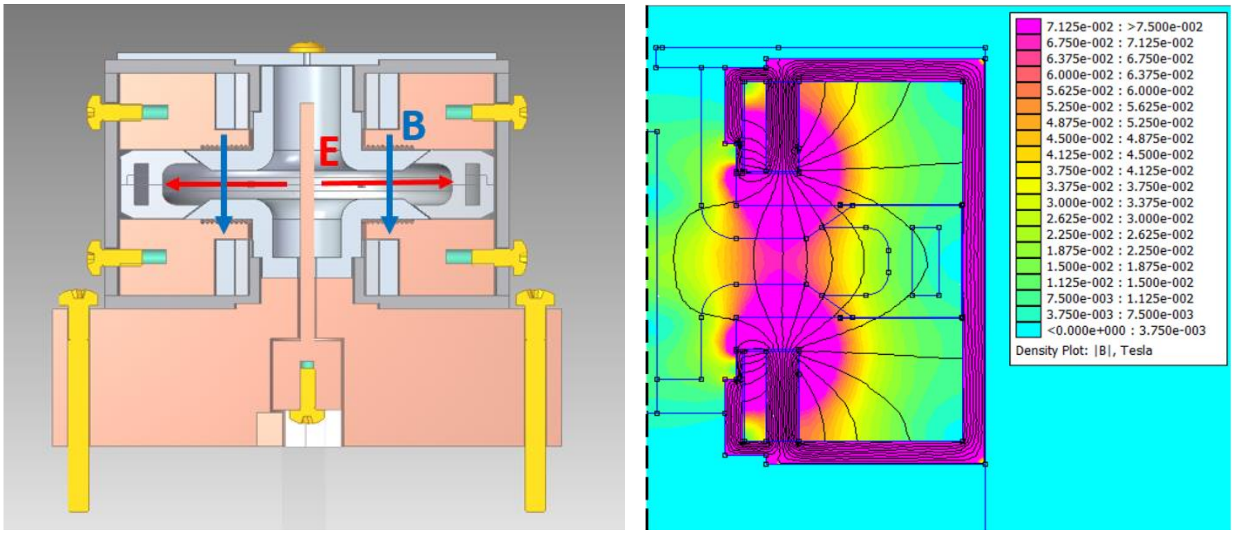

Figure 1. Annular magnets assembly: (left) section of the Hall-type neutralizer with electric and magnetic fields shown, (right) axisymmetric magnetic field inside the neutralizer simulated with FEMM.[10,11]

The neutralizer consists of an annular stainless steel cathode, from which the working gas is introduced into the discharge volume, a pin copper anode that extends along the axis of symmetry of the device, and a magnetic circuit made by a magnetic core structure and permanent magnets. As listed in Table 1, three magnetic configurations have been tested: (i) an annular magnets assembly that produces a closed-loop Hall current, (ii) an arc magnets assembly that causes four open-loop Hall currents, (iii) and a third magnet configuration that consists of the annular magnet assembly coupled with an electromagnet located in proximity of the extraction orifice. Electrons are extracted through an orifice of diameter of 1.8 mm and axial length of 1.8 mm.

Table 1. Hall-type neutralizer configurations.

Assembly Part / Configuration	Annular magnets	Arc magnets	Extraction Electromagnet
1	X		
2		X	
3	X		X

1. Annular magnets assembly

The first magnet assembly consists of annular magnets whose magnetic field drives a closed-loop Hall current along the azimuthal direction. A section view of the closed-loop Hall current neutralizer where the electric and magnetic fields are depicted, and the magnetic field contour plot simulated within the device are shown in Figure 1. A more detailed discussion of this design is covered elsewhere.[11] This setup corresponds to configuration 1 in Table 1.

2. Arc magnets assembly

The second magnet assembly consists of four arc magnets whose axial polarity is alternated. This magnetic configuration allows the creation of four open-loop Hall currents and four null regions within the neutralizer. Lateral and top views of this assembly are shown in Figure 2. In Figure 2 it is also shown the magnetic field directions and the resulting $\boldsymbol{E} \times \boldsymbol{B}$ drifts. The contour plots of the magnetic field at three different planes intersecting the magnetic circuit are shown in Figure 3, where the intersecting plane is depicted at the bottom left corner of each plot. The middle and bottom plots clearly show the magnetic null

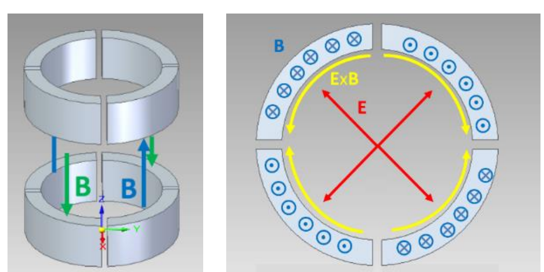

Figure 2. Arc magnet assembly: (left) lateral view showing the magnetic field directions, and (right) top view showing the resulting $\boldsymbol{E} \times \boldsymbol{B}$ drifts.

region as seen in the planes along and across it, respectively. The classical diffusion coefficient across a magnetic field is

$$D_{\perp} = D/[1 + (\omega_c \tau_m)^2] \quad (2)$$

where D is the diffusion coefficient in absence of a magnetic field, ω_c is the gyration frequency and τ_m is the characteristic time between electron momentum transfer collisions. Since $D > D_{\perp}$, the four null regions facilitate the electron diffusion along the radial direction of the neutralizer.

Electrons are temporary trapped in the strong magnetic field region, enhancing the probability of ionizing collisions with neutrals. Due to the presence of a radial electric field, electrons drift along the $\boldsymbol{E} \times \boldsymbol{B}$ directions. It is expected that at the beginning of the $\boldsymbol{E} \times \boldsymbol{B}$ regions, corresponding to the tails of the $\boldsymbol{E} \times \boldsymbol{B}$ arrows shown in the right illustration in Figure 2, the electron population has a lower density than at the end of the drift, corresponding to the head of the $\boldsymbol{E} \times \boldsymbol{B}$ arrows. At this point a higher number of electrons can diffuse radially along the null-regions and, subsequently, be extracted from the neutralizer. This configuration is expected to reduce the resistivity of the plasma by facilitating electron mobility along well defined paths and, thus, lowering the voltage needed to sustain the discharge.

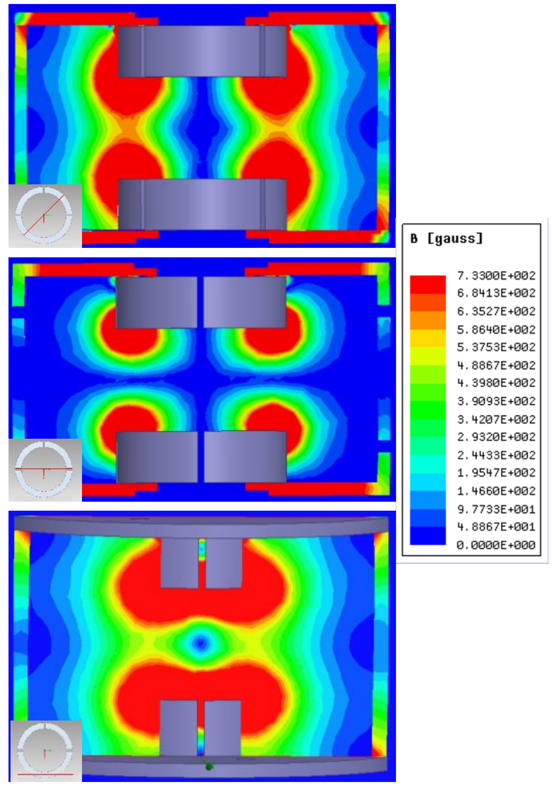

Figure 3. Contour plots of the magnetic field at three planes intersecting the arc magnet assembly at (top) centre of the arc magnet, (middle) along the null region, and (bottom) across the null region.

3. Extraction Electromagnet

In some of the tests performed with the annular magnets assembly, an electromagnet was attached on the extraction plate. The electromagnet is supported by an aluminium structure that has an orifice of 3 mm in diameter extending axially for 8.1 mm. This orifice is coaxial to the extraction orifice, thus, permitting electron extraction through a channel long 9.9 mm (extraction orifice plus electromagnet structure). A peak axial magnetic field of about 100 G is generated inside the extraction channel (see Figure 4). This magnetic field has the effect to reduce the electron Larmor radius to values lower than the extraction orifice radius. The purpose of the electromagnet is to funnel electrons toward the orifice, thus, facilitating their extraction.

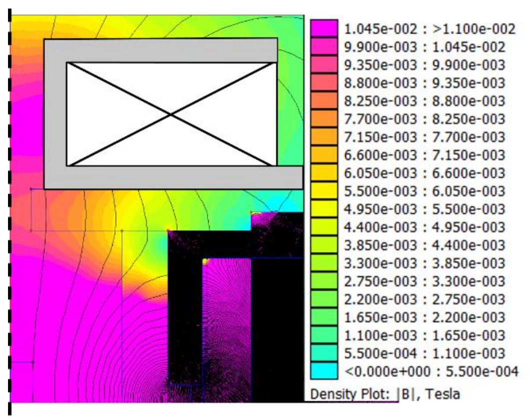

Figure 4. Close up of the axisymmetric magnetic field contour plot at the extraction region simulated with FEMM.[11] The plot shows the superposition of the magnetic field generated by the electromagnet and the permanent annular magnets.

B. Magnetron Neutralizer

1. Magnetron planar discharge

Magnetron planar discharges are DC-magnetized plasma sources typically used for sputter deposition of metallic thin films or etching. The plasma discharge takes place between two planar parallel electrodes, which are the cathode and the anode of the system. Almost all of the anode-cathode voltage appears at the cathode sheath, accelerating ions towards the wall and balancing the electron current collected at the anode. As a consequence, the electric field is shielded through the remaining part of the gap. The discharge is sustained mainly by secondary electron emission from the cathode. Secondary electrons gain energy throughout the sheath potential ramp and ionize the neutral background gas by electron-neutral collisions. A cusped-field magnetic field is used at the cathode in order to operate the discharge at lower voltages, lower pressures, and higher current density in comparison with standard glow discharges. The magnetic field presents a predominant axial component at the magnetic poles and a radial component in the intermediate region. The latter, in combination with the axial electric field, generates an azimuthal $\boldsymbol{E} \times \boldsymbol{B}$ closed electron drift, enhancing electron confinement and boosting the ionization.

A high density plasma ring forms in the $\boldsymbol{E} \times \boldsymbol{B}$ region embedded in a lower density plasma.[12] The ring width can be related to the electron Larmor radius r_{ce} (in this case $r_{ce} = \sqrt{2m_e V_D/e}/B$) and the field line curvature R_c as

$$w \approx 2(2r_{ce}R_c)^{1/2} \tag{3}$$

The ions are unmagnetized and their flow to the cathode is described by the Child-Langmuir theory, which provides an upper limit to the ion current density to the cathode surface:

$$J_i = 4/9\, \epsilon_0 (2e/M_i)^{1/2}\, V_D^{3/2}/s^2 \tag{4}$$

where e is the elementary charge, M_i the ion mass, m_e the electron mass, V_D the discharge voltage (which is assumed to appear entirely at the cathode sheath) and s the sheath thickness. The current density can be expressed as a function of the plasma ring radius R and thickness w:

$$J_i = I_D/(2\pi R w) \tag{5}$$

where I_D is the discharge current. Therefore the topology and intensity of the magnetic field has a critical role in maximizing the current density at a given discharge voltage.

2. Design

This peculiar plasma source configuration has been exploited to generate a high density plasma bounded between two electrodes. Electrons are extracted through a set of orifices on the anode.

A magnetron-type cavity has been designed based on the previous theory and relations. During the design process, the following was taken into consideration: (i) in the radial magnetic field region (i.e. the highest ionization annular volume), the field lines run parallel to the cathode surface in order to further decrease electron cross-field diffusion and facilitate trapping of electrons within the sheath; the aim is to partially neutralize the sheath and reduce its thickness in order to improve the achievable ion current density; (ii) the neutral gas is injected in a counter-streaming configuration in order to increase the neutral resident time within the magnetron cavity and improve the propellant utilization; (iii) the flexible design allows a quick change of the geometrical parameters of the source: discharge gap thickness, number and diameter of holes on the extraction plate (which determine the internal neutral pressure for a given mass flow rate), number of the neutral gas injection ports.

The 3D section view and a picture of the magnetron neutralizer are shown in Figure 5 and Figure 6, respectively. The magnetron supporting structure is made of polytetrafluoroethylene (PTFE). The choice of this material is a trade-off between cost and mechanical properties. PTFE presents a working temperature up to 250ºC and a relatively low cost. The supporting structure presents grooves to house SmCo magnets. Samarium cobalt presents a maximum operating temperature up to 300-350ºC and an excellent thermal stability. Finite-element magnetostatic simulations have been performed to tailor the magnetic field topology to the geometry. The cathode and the anode electrodes are made of aluminium. A borosilicate glass cylinder encloses the plasma discharge. The sealing of the plasma enclosure is obtained by O-rings located at the interfaces between the various components.

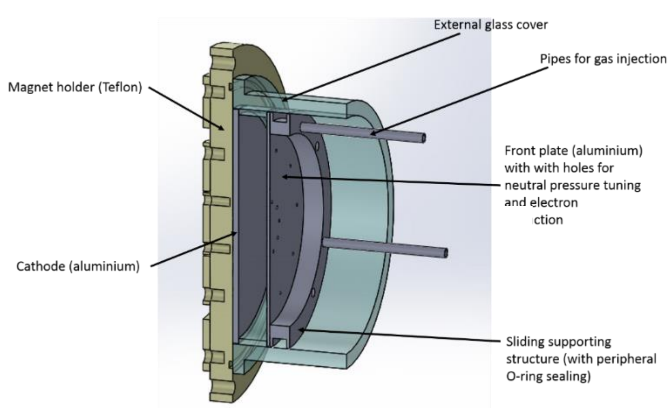

Figure 5. CAD model of the magnetron neutralizer.

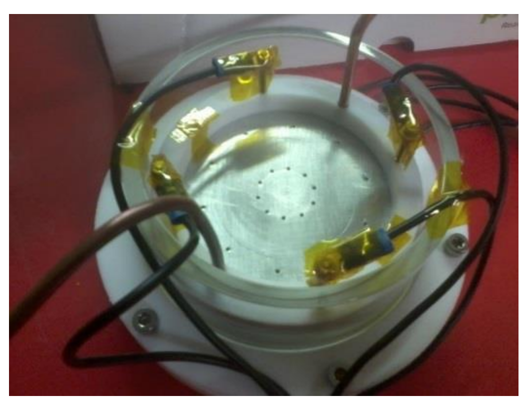

Figure 6. Magnetron neutralizer assembly.

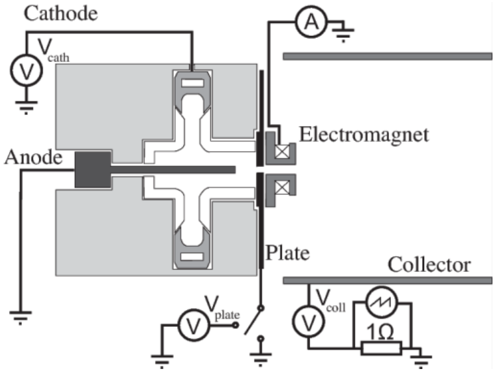

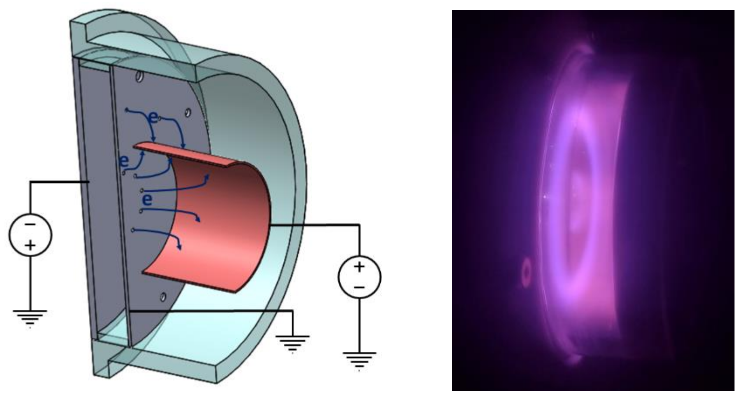

Figure 7. Electrical schematic of the Hall-type neutralizer experimental setup.

Figure 8. (left) Simplified section view of the neutralizer and collector with the electrical connections and (right) plasma discharge during the tests with argon.

III. Experimental Campaign

A. Experimental Equipment

The experiments have been performed in Hermes vacuum chamber at the Surrey Electric Propulsion Laboratory. The pumping system, comprised of an oil diffusion pump, has a capacity of about 2000 l/s and throughput of about 4 Torr-l/s. The base pressure is 10^{-5} mbar. The laboratory equipment consists of four power supplies, a Glassman High Voltage Inc. model EQ50R24 (5000 V, 240 mA), a Sorensen DCS300- 4E (300 V, 4 A), a Sorensen SGA1000-5 (1000 V, 5 A) and a TTi CPX200DP, a Tektronix TDS2024B oscilloscope, a RS thermocouple reader model 615-8212, and a Bronkhorst EL-FLOW® Select model F-201CV mass flow controller. Two thermocouples are used to monitor the temperature in proximity of the permanent magnets.

B. Hall-Type Neutralizer Setup

A schematic of the electrical connections used in the Hall-type neutralizer is shown in Figure 7. The cathode is powered by the Glassman (5000 V, 240 mA) power supply and it is controlled in current limited mode. The pin anode is connected to ground. The extraction plate and, when mounted, the holding structure of the electromagnet are grounded, floated, or voltage-controlled by the TTi CPX200DP power supply. Electrons are extracted by means of an external cylindrical collector of internal diameter of 7.6 cm and axial length of 10 cm. The collector is connected to the Sorensen DCS300- 4E (300 V, 4 A) power supply which is operated in voltage limited mode. The electromagnet has 25 turns of a Ø1.5 mm copper wire, internal diameter of 5 mm and axial length of 7 mm. The winding is powered by the TTi CPX200DP power supply at a current of 4.1 A. The DC Hall-type neutralizer is tested with Ar, Kr, and air.

C. Magnetron Neutralizer Setup

The magnetron discharge is powered by the Glassman (5000 V, 240 mA) power supply. The cathode is negatively polarized and the extraction plate (anode) is connected to the system ground. The extracted electron current is drawn through a collector by the Sorensen SGA1000-5 (1000 V, 5 A). Since the extraction plate presents two concentric arrays of orifices, we have used a tube-shaped copper collector with an intermediate diameter between the extraction orifices arrays diameters. The outer surface of the tube collects electrons from the outer array, the inner surface from the inner array. The collector is electrically insulated from the extraction plate. A schematic of the electrical connections is shown in Figure 8 along with the neutralizer during the tests inside Hermes chamber. The magnetron neutralizer is tested with He, Ar, Xe, and air.

D. Performance Metrics

The neutralizers' current and voltage have been monitored during tests without electron extraction and plotted as I-V characteristics. When electron extraction is performed, also the collector current is recorded. The performance parameters derived are the extraction parameter α, the partial power efficiency H_p, and the gas utilization factor U defined as

$$\alpha = I_{extr}/I_D \tag{6}$$

$$H_p = I_{extr}/P_D \quad (7)$$

$$U = I_{extr}/(C\,\dot{m}_g) \quad (8)$$

where I_{extr} is the extracted electron current measured at the collector, I_D is the discharge current, $P_D = I_D V_D$ is the discharge power, V_D is the discharge voltage, $C = 0.07174\ \mathrm{A/sccm}$ is a constant, and $\dot{m}_g$ is the propellant flow rate in sccm.

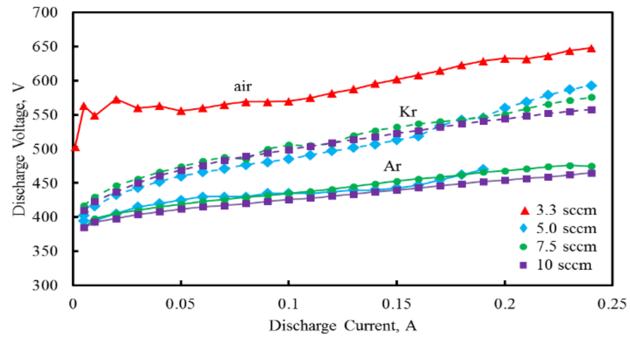

Figure 9. I-V characteristics of the DC Hall-type neutralizer with arc magnets using Ar, Kr, and air at various flow rates.

IV. Results and Discussions

A. Hall-Type Neutralizer

In a previous publication,[11] we have already discussed the experimental results of configuration 1 which successfully operated with He, Ar, Xe, air, and water vapour. In the following sections, we present the preliminary results of the experiments performed with configuration 2 and 3.

1. *Configuration 2*

The *I-V* characteristics of the DC Hall-type neutralizer tested with Ar, Kr, and air are shown in Figure 9. Argon and krypton flow rates are 5, 7.5, and 10 sccm, while air has a flow rate of 3.3 sccm. The discharge current is increased up to 0.24 A. Generally, for each atomic gas the trend of the three flow rate curves is similar irrespective of gas flow rate, with small variation among them. However, the curves remarkably separate when the gas type is changed. The argon discharge maintains the lowest voltage, which is between 380-470 V. The krypton curves vary between 400-590 V. Finally, with air the *I-V* characteristic extends from 500 V to 650 V.

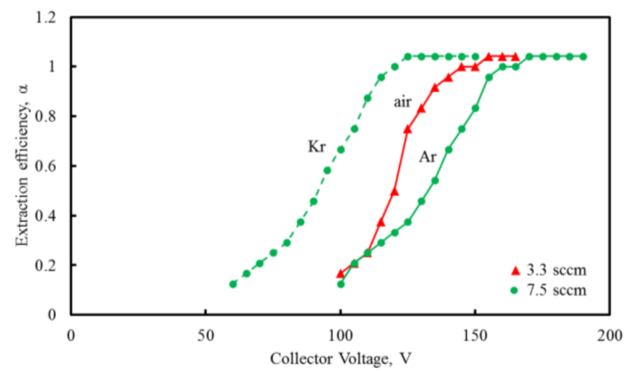

Figure 10. Extraction efficiency versus external collector voltage of the DC Hall-type neutralizer at a discharge current of 0.24 A.

The plots of the extraction efficiency versus the collector voltage are shown in Figure 10. The flow rate of Kr and Ar is 7.5 sccm, while the air flow rate is 3.3 sccm. All plots are shown for a discharge current of 0.24 A. Extraction saturation is reached for all three gases at slightly different collector voltages.

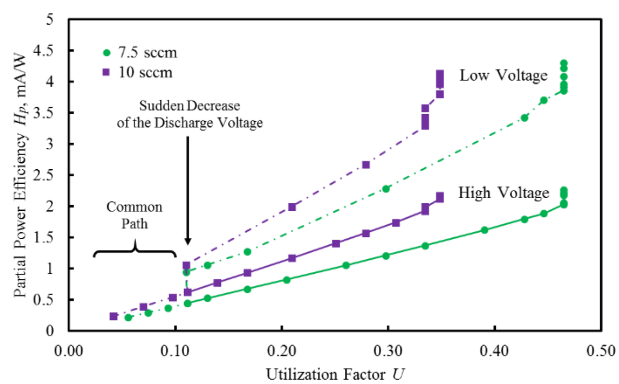

Figure 11. H_p-U plots for Kr showing the effect of the arc magnets configuration in the DC Hall-type neutralizer.

The effect of the arc magnets configuration on the discharge is visible in Figure 11, where the H_p-U plots are shown for Kr at flow rates of 7.5 and 10 sccm, and discharge current of 0.24 A. When the discharge is initiated and electrons are extracted, the H_p-U plot may follow two paths: the high voltage path (shown in solid lines), and a low voltage path (shown in dash-dot lines). In the latter case, at the beginning of the extraction, therefore at low H_p and U values, H_p rises proportionally with U as the extracted electron current increases. At a value of the utilization factor equal to 0.11, the discharge voltage drops by 200-240 V, causing a steep rise of the partial power efficiency. From this point, the discharge is stable at lower discharge voltage values, and, thus, the H_p-U plots follow the low voltage path. This behaviour of the discharge was not observed in previous tests of the annular magnet configuration.

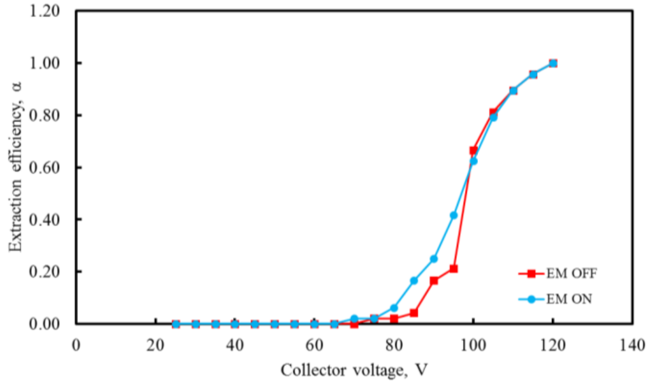

Figure 12. Configuration 3: extraction efficiency versus collector voltage for flow rate of Ar of 5 sccm, and discharge current of 0.24 A.

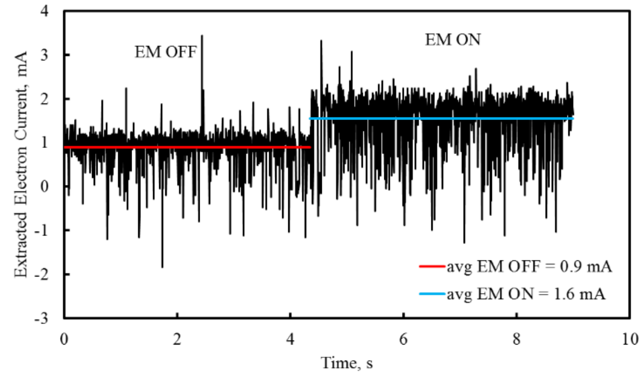

Figure 13. Example of extraction enhancement: extracted electron current before and after the electromagnet (EM) is turned on.

2. *Configuration 3*

The extraction efficiency versus collector voltage for Ar at flow rate of 5 sccm and discharge current of 0.24 A is shown in Figure 12. The plot shows the effect of the extraction electromagnet. The presence of an axial magnetic field within the exit orifice enhances electron extraction at collector voltages in the 80-95 V range. The magnetic field has not effect for an extraction efficiency higher than 0.5.

The dynamic behaviour of the extracted electron current has been measured through a shunt resistor and an oscilloscope.

The axial magnetic field has three effects on the extracted electron current. As described earlier, the first effect is to increase the amount of electrons extracted from the neutralizer within a certain collector voltage range. This is shown in Figure 13, where the raw data of the extracted electron current are presented along with the average current before and after the electromagnet is turned on. The second effect is to reduce the amplitude of the current fluctuations of the extracted electron current, as shown in Figure 14. Finally, the third effect is to assist the transition from pulsed to continuous electron extraction, as shown in Figure 15. Pulsed electron extraction is observed when the electric field produced by the collector is just strong enough to reduce the potential barrier within the extraction orifice and start a plasma bridge between the plasma inside the neutralizer and the collector.

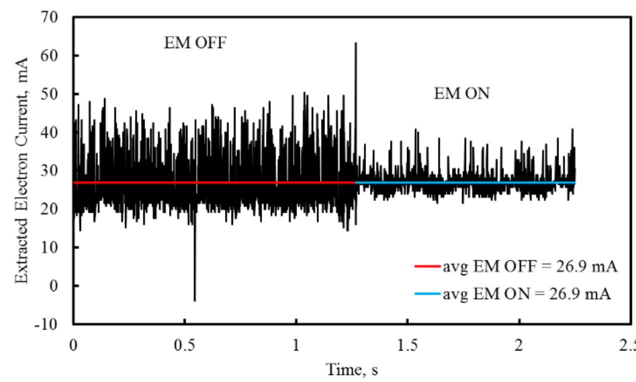

Figure 14. Example of extracted current oscillation reduction: extracted electron current before and after the electromagnet (EM) is turned on.

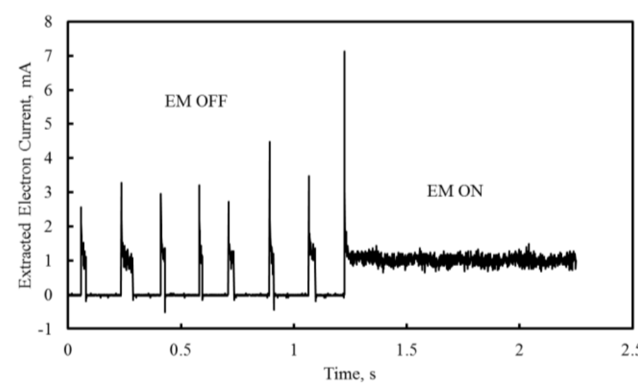

Figure 15. Example of transition from pulsed to continuous extraction when turning on the electromagnet.

B. Magnetron Neutralizer

Figures 16-18 illustrate several extraction characteristics of the neutralizer operated with xenon. The voltage needed to trigger the electron extraction is 25 V. Extraction factors equal to 1 are obtained and, in some cases, the extraction factor is higher than unity due to additional ionization taking place outside the neutralizer. As shown in Figure 17, the trend of the current through the extraction plate is monotonically decreasing for increasing extracted current and reaches a null value when the extraction factor is equal to 1. When the latter factor is higher than unity the additional electron current is pull out from the extraction plate in order to satisfy the conservation of current balance. In general, we do not observe a significant influence of the cathode current and mass flow on the extraction characteristic.

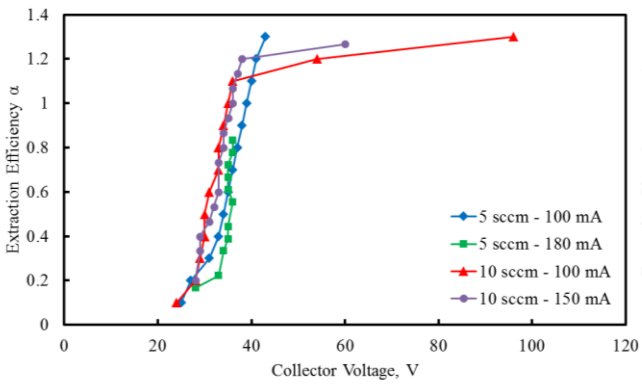

Figure 16. Extraction efficiency versus collector voltage of the magnetron neutralizer in DC-only mode operated with xenon.

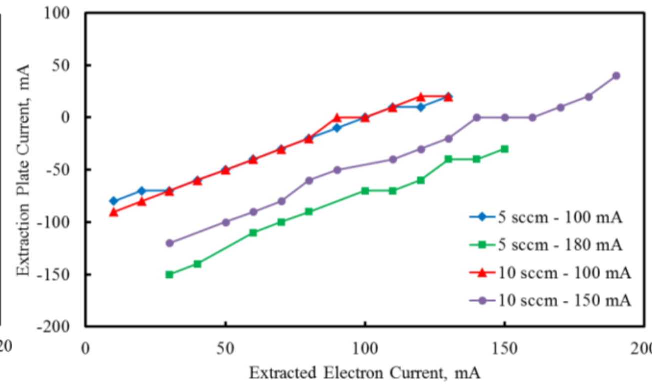

Figure 17. Extraction plate current versus extracted electron current of the magnetron neutralizer in DC-only mode operated with xenon.

At $\alpha = 1$, an energy efficiency of 3 mA/W is calculated for xenon, and the maximum propellant utilization factor is 0.45. The trend of the energy efficiency as a function of the propellant utilization factor is shown in Figure 18. The trend matches that one observed for the Hall-type neutralizer, yielding similar comments and conclusions.[11] This similarity originates from the basic physical principles which govern the two discharges, which have been described in the previous sections.

Table 2 summarises the performance metrics for different propellants. The data have been gathered during extensive test campaigns with or without external collector for electron extraction. In the latter case an extraction factor equal to unity has been assumed for calculating the metrics.

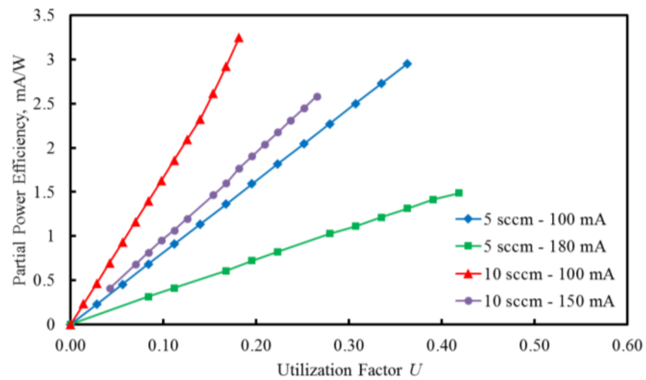

Figure 18. Partial power efficiency versus utilization factor of the magnetron neutralizer in DC-only mode operated with xenon.

Table 2. Performance metrics of the magnetron neutralizer

	He	Ar	Xe	air
Maximum Partial Power Efficiency [mA/W]	5.3	5.6	4	3.2
Maximum Utilization Factor U	0.6	3.4	0.4	0.2

V. Conclusions

Two different neutralizers have been investigated, a Hall-type neutralizer in which ionization is enhanced by the action of a $\boldsymbol{E} \times \boldsymbol{B}$ current, and a magnetron configuration. The neutralizers have been extensively characterized and their operating and performance envelopes have been determined for a broad range of test conditions.

Several propellants have been used during the test campaign, demonstrating the capability of the neutralizers to operate both with noble gases and with molecular mixtures. In particular the following gases have been used: He, Ar, Kr, Xe, and air.

The Hall-type neutralizer has been tested in three configurations, depending on the assembled magnetic circuit: including annular magnets (configuration 1), arc magnets (configuration 2), and annular magnet with extraction electromagnet (configuration 3). Results from tests on configuration 2 demonstrate that the discharge voltage drops by 200-240 V when electrons are extracted, with respect to a discharge without electron extraction. This behaviour was not observed in previous tests performed on configuration 1. The superposition of an axial magnetic field through the extraction orifice (configuration 3) introduces an improvement in electron extraction within a mid-low collector voltage range, a reduction of the amplitude of extracted electron current fluctuations, and aids the transition from pulsed to continuous electron extraction when the dominant extraction mode is pulsed.

The magnetron neutralizer has extraction trends similar to those observed for the Hall-type neutralizer, yielding similar comments and conclusions. This similarity originates from the basic physical principles which govern the two discharges. A summary of the performance metrics are shown for He, Ar, Xe and air.

Depending on the working gas, the DC configurations tested in this study show a maximum power efficiency of 3-5 mA/W and gas utilization factor up to 3.4. In comparison, the state-of-the-art thermionic hollow cathodes reach power efficiency of 47.6 mA/W and gas utilization of 83.6. Although conventional hollow cathodes show higher efficiency with regard to the laboratory-model presented in this study, plasma cathodes have the advantage to operate with molecular propellants that chemically react with and degrade electron emission of thermionic materials.

Acknowledgments

This work is part of the strategic partnership between University of Surrey and Airbus Defence and Space. This research was conducted under innovation funding from Airbus Defence and Space. The authors would like to thank Surrey Satellite Technology Ltd for sponsoring the PhD studentship that enabled part of this research to be conducted. A. Gurciullo also thanks the Institution of Mechanical Engineers for supporting his participation at the conference.

References

[1]Cronin, J. L., "Practical Aspects Of Modern Dispenser Cathodes," *Microwave Journal*, 1979.

[2]Gallagher, H. E., "Poisoning of LaB6 cathodes," *Journal of Applied Physics*, vol. 40, 1969, pp. 44–51.

[3]Szabo, J., Robin, M., Paintal, S., Pote, B., and Hruby, V., "High Density Hall Thruster Propellant Investigations," *48th AIAA/ASME/SAE/ASEE Joint Propulsion Conference & Exhibit*, AIAA 2012-3853, Atlanta, Georgia, 2012.

[4]Charles, C., Boswell, R. W., Laine, R. and MacLellan, P., "An experimental investigation of alternative propellants for the helicon double layer thruster," *Journal of Physics D: Applied Physics*, vol. 41, n. 17, p. 175213, 2008.

[5]Oks, E., *Plasma Cathode Electron Sources*, Weinheim, Germany: WILEY-VCH Verlag GmbH & Co. KGaA, 2006.

[6]Godyak, V., Raites, Y., and Fisch, N. J., "RF plasma cathode-neutralizer for space applications," *30th International Electric Propulsion Conference*, Florence, Italy, 2007.

[7]Diamant, K. D., "Resonant Cavity Hollow Cathode," *41st AIAA/ASME/SAE/ASEE Join Propulsion Conference and Exhibit*, Tucson, Arizona, 2005.

[8]Kamhawi, H., Foster, J. E., and Patterson, M. J., "Operation of a Microwave Electron Cyclotron Resonance Cathode," *40th AIAA/ASME/SAE/ASEE Joint Propulsion Conference and Exhibit*, Fort Lauderdale, Florida, 2004.

[9]Longmier, B., Baalrud, S., and Hershkowitz, N., "Nonambipolar electron source," *Review of Scientific Instruments*, vol. 77, n. 11, p. 113504, 2006.

[10]Meeker, D. C. (Dec. 3, 2006). Finite Element Method Magnetics, Version 4.0.1. [Online]. Available: http://www.femm.info

[11]Gurciullo, A., Lucca Fabris, A., and Knoll, A., "Direct Current Plasma Electron Source for Electric Propulsion Applications Using Atomic and Molecular Propellants," *IEEE Transactions of Plasma Science*, vol. 45, 2017, pp. 2472–2480.

[12]Lieberman, M. A., and Lichtenberg, A. J., *Principles of Plasma Discharges and Material Processing*, Hoboken: John Wiley & Sons, Inc, 2005.